ELSEVIER

Chemical Geology 236 (2007) 350–366

CHEMICAL GEOLOGY
INCLUDING
ISOTOPE GEOSCIENCE

www.elsevier.com/locate/chemgeo

Origin and age of pore waters in an actively venting gas hydrate field near Sado Island, Japan Sea: Interpretation of halogen and ^{129}I distributions

Hitoshi Tomaru [a,*], Zunli Lu [a], Glen T. Snyder [b], Udo Fehn [a], Akihiro Hiruta [c], Ryo Matsumoto [c]

[a] *Department of Earth and Environmental Sciences, University of Rochester, Rochester, NY, 14627, USA*
[b] *Department of Earth Science, Rice University, Houston, TX 77005, USA*
[c] *Department of Earth and Planetary Science, University of Tokyo, Tokyo 113-0033, Japan*

Received 19 July 2006; received in revised form 28 September 2006; accepted 12 October 2006

Editor: P. Deines

Abstract

A gas hydrate field with highly active venting of methane was recently found near Sado Island in the eastern Japan Sea. Piston cores were collected from active venting sites and nearby locations in the Umitaka Spur–Joetsu Knoll area during two cruises in 2004 (UT04) and 2005 (KY05-08). We report here halogen concentrations and $^{129}I/I$ ratios in pore waters associated with gas hydrates from these expeditions. The strongly biophilic behavior of I and, to a lesser degree, of Br together with the presence of the long-lived iodine radioisotope (^{129}I) allow evaluation of potential source materials for methane in gas hydrate systems. Depth profiles of all three halogens, particularly the very rapid downward increases of Br and I concentrations, strongly suggest input of deep fluids enriched in Br and I, but the profiles also display the effects of gas hydrate formation and dissociation. Although the $^{129}I/I$ ratios are modified by ^{129}I from seawater and sediments at shallow depth, likely ratios of the deep fluids are estimated to be between 400×10^{-15} and 600×10^{-15}, equivalent to a Late Oligocene to Early Miocene age. Ages in the active methane venting sites typically are closer to the old end of this range than those in the reference sites. This age range suggests that the methane associated with venting and gas hydrate formation in this area is derived from organic materials accumulated during the initial opening of the Japan Sea. The Umitaka Spur–Joetsu Knoll gas hydrate field demonstrates the movement of deep fluids associated with the release of significant amounts of methane from the seafloor, processes which might be important components of mass transfer and carbon cycle in the shallow geosphere.

Keywords: Pore water; Halogen; ^{129}I; Gas hydrate; Japan Sea

1. Introduction

Gas hydrate fields are commonly found in deep sandy sediments as “disseminated gas hydrate” filling sediment pores (Uchida et al., 2004; Tréhu et al., 2004), which generally are identified by bottom simulating reflectors

* Corresponding author. Tel.: +1 585 275 2514; fax: +1 585 244 5689.
E-mail address: hitoshi@earth.rochester.edu (H. Tomaru).

0009-2541/$ - see front matter © 2006 Elsevier B.V. All rights reserved.
doi:10.1016/j.chemgeo.2006.10.008

(BSRs) indicating the lower boundary between gas hydrate and free gas layers. In addition to the "disseminated" occurrences, an increasing number of near-surface "massive gas hydrate" deposits has been discovered in continental margins and inland lakes, which are associated with rapid methane transport by gas, mud, or fluid expulsion (e.g. Ginsburg et al., 1999; Suess et al., 1999; Mazurenko et al., 2003; Haeckel et al., 2004; Hensen et al., 2004; Shoji et al., 2005). The latter phenomenon is the consequence of an unusually high and localized flux system, which typically releases a large amount of methane into the overlying water column and might be an important link in the shallow carbon cycle.

The Umitaka Spur–Joetsu Knoll area, southwest of Sado Island in the eastern margin of the Japan Sea, is a region where large-scale methane venting on the seafloor has been identified in echosounder images (Aoyama et al., 2005). The methane plumes reach diameters of 100 m and heights of 200 to 700 m and cause an increase in the concentration of dissolved methane in seawater to levels as high as 160 nmol/L (Ishida et al., 2005). During the expeditions of R/V Umitaka-maru of the Tokyo University of Marine Science and Technology in 2004 (UT04) and R/V Kaiyo of the Japan Agency for Marine-Earth Science and Technology (JAMSTEC) in 2005 (KY05-08), intensive piston coring programs were carried out in this area. Thick layers of massive gas hydrates, ~2.6 m, were recovered in the upper 12 m below seafloor (mbsf) around the sites on the spur and the knoll where rough seafloor with carbonate clasts and outcropping gas hydrates are observed by the deep-tow camera of R/V Kaiyo (Matsumoto et al., 2005). These results indicate strong linkage between continuous large methane supply and methane-induced carbon storing in carbonates and gas hydrates. Origin and accumulation of the methane, however, are not well known, which are processes, essential for the understanding of gas hydrate systems associated with active methane seepage.

Recent investigations of halogen concentration together with the determination of $^{129}I/I$ ratios have been useful to identify the potential ages and source formations of the fluids in gas hydrate systems (Fehn et al., 2000, 2003, 2006; Tomaru et al., 2006a). In this study we focus on the halogen geochemistry and $^{129}I/I$ ratios of pore waters collected from the Umitaka Spur–Joetsu Knoll area, for the determination of origin of methane in the gas hydrate system in the backarc marginal basin of the Japanese Island Arc. The study area has been geologically active during the formation of the Japan Sea and is close to the region with the largest hydrocarbon deposits in Japan. The age signal associated with the gas hydrates will contribute to the understanding of the depositional history of sequences associated with the formation of the present Japanese Island Arc and of the origin of hydrocarbons in this area.

2. Iodine geochemistry

Iodine has the most biophilic nature of the major halogens (Cl, Br, and I), and its behavior is very different from chlorine, the least biophilic of these three. Bromine has characteristics somewhat between the other two elements and is commonly examined together with I and Cl. The largest reservoirs of Cl and I at the earth surface are seawater (2.66×10^{13} t, 72.2% of total Cl) and marine sediments (5.90×10^{12} t, 68.2% of total I), respectively (Muramatsu and Wedepohl, 1998). The latter reflects the extensive enrichment of I in marine phytoplankton and algae compared to seawater and the subsequent accumulation in marine sediments (Tsunogai, 1971; Price and Calvert, 1977; Elderfield and Truesdale, 1980; Harvey, 1980). Although the dominant ionic dissolved species of I in seawater is iodate (IO_3^-) (Tsunogai, 1971), iodide (I^-), iodine (I_2), or iodate (IO_3^-) can exist depending on the redox condition in sediments. In oxic sediments, decomposition of organic materials liberates I^- into the aqueous phase and the I^- is oxidized to IO_3^- and I_2. These species are incorporated into the organic detritus again, leading to an increase of I at the sediment–water interface in the shallow oxic zone (Kennedy and Elderfield, 1987a,b). In anoxic sediments at depths, reduced I^- is released from sediments to the aqueous phase, resulting in I^- enrichment in pore waters. The variation of dissolved bromine in pore water compared to seawater is generally smaller than that of iodine because bromide (Br^-) is the only stable species during diagenesis or in organic materials. Although there are only few studies available on Br^- behavior in such systems, the amount of organic carbon correlates well with Br^- concentrations (Price et al., 1970; Price and Calvert, 1977), reflecting Br^- release form organic materials during diagenesis along with iodine.

Iodine has one stable isotope (^{127}I) and a long-lived radioisotope (^{129}I) with a half-life of 15.7 Myr. In nature, ^{129}I is mainly produced by the spallation reaction of Xe in the atmosphere and by the spontaneous fission of ^{238}U in the earth's crust. Both of these processes contribute similar amounts to the ^{129}I budget in the ocean (Fabryka-Martin et al., 1985). Because of the long residence time of iodine in the ocean (~300,000 yr; Broecker and Peng, 1982) and rapid ion exchange among ocean, biosphere, and atmosphere, (Moran et al., 1998), the pre-anthropogenic iodine isotopic composition has been homogeneous in surface reservoirs with a ratio of radioactive ^{129}I to stable ^{127}I ($^{129}I/I$) of $(1500\pm150)\times10^{-15}$ (Moran

et al., 1998; Fehn et al., in press). Releases of large quantities of anthropogenic ^{129}I from nuclear bomb tests, nuclear accidents, and reprocessing plants have disturbed the isotope equilibrium in surface reservoirs, but have not reached depths beyond the layer of bioturbation in marine sediments (Moran et al., 1998). Due to the development of accelerator mass spectrometry (AMS) for the determination of $^{129}I/I$ ratios (Elmore et al., 1980), the ^{129}I system can be applied for geological investigations with an age range of 80 Ma (Sharma et al., 2000).

3. Geological setting

The Japan Sea is a semi-isolated marginal basin which is surrounded by the Japanese Island Arc and the Asian main land (Fig. 1A), and was formed by the westward rift propagation initiated at a major strike–slip fault between the Eurasian (Amur) and North American (Okhotsk) Plates during the Early to Middle Miocene (Jolivet and Tamaki, 1992). Although the entire Japan Sea was extending between 32 to 10 Ma, major opening and formation of the Japan Sea, accompanied by a large submarine eruption of volcanic rocks called Green Tuff, occurred between 28 and 18 Ma, resulting in rapid deposition of thick marine sediments (Yamaji, 1990; Tamaki et al., 1992; Taira, 2001). After 18 Ma, the extension continued to be active only in the northeastern margin of the Japan Sea, the anti-clockwise and clockwise rotations of NE and SW geological parts of Japan formed a sedimentary basin across the main island of Japan, Fossa

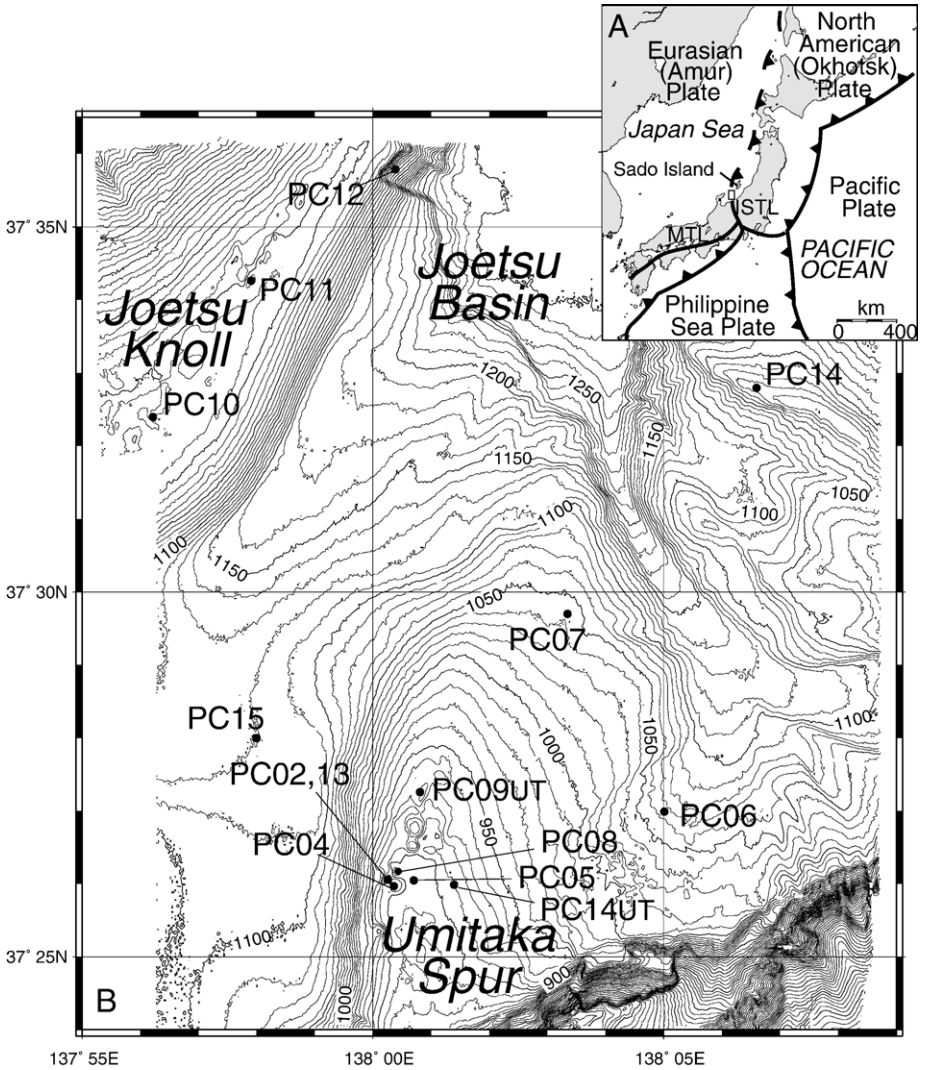

Fig. 1. (A) Geological setting of Japan. Box represents the location of the Umitaka Spur–Joetsu Knoll gas hydrate field in panel B. (B) Detailed map of research area. Black dots indicate piston core sampling sites during UT04 and KY05-08 cruises.

Magna, which is located in the southern end of the Miocene rift system and filled with thick (>6000 m) and strongly folded Miocene marine sediments (Kato, 1992). The Itoigawa–Shizuoka Tectonic Line (ISTL) bounds the western edge of the Fossa Magna, and probably runs just west of the research area in an N–S direction (Fig. 1A). At ~15 Ma, spreading of the Japan Sea ceased and the plate setting was settled close to the present position, but the Philippine Sea Plate motion led to activation of the ISTL at 6 Ma and of the Median Tectonic Line (MTL) at 5 Ma (e.g. Matsubara and Seno, 1980; Jolivet et al., 1994). The east–west directed convergence initiated an incipient subduction along the eastern margin of the Japan Sea at <1 Ma (e.g. Nakamura, 1983; Tamaki and Honza, 1985; Okamura et al., 1995).

The research area is characterized by three rises, the Umitaka Spur, northern part of the Joetsu Knoll, and a small ridge in the east of the Joetsu Basin continuing to the Toyama Trough (Fig. 1B), a northern extension of the ISTL to the northwest of the area (Nakamura, 1983). These rises are mainly composed of mud to gravel of the Quaternary Takada-oki Group (Okamura et al., 1994). The underlying Neogene Joetsu-oki Group of mudstone to conglomerate crops out only at the highly deformed anticline of the Umitaka Spur, where these young sediments reach a thickness of >4000 m. The acoustic basement of igneous and hardly lithified sedimentary rocks beneath the Joetsu-oki Group is exposed only along the western slope of the Yoneyma-Ogi uprifts, northeast of this area (Okamura et al., 1994).

The Japanese petroleum explorations by the Ministry of Economy, Trade and Industry (METI) and Japan Oil, Gas and Metals National Corporation (JOGMEC) in 2003 and 2004 identified prominent BSRs at depth of ~170 mbsf, indicating the presence of deep-seated gas hydrates, and chaotic sediment structures under large depressions (pockmarks) in the seismic profiles on the spur, demonstrating the presence of gas-charged sediments (Matsumoto et al., 2005). High resolution topographic images exhibit NNE–SSW trending large pockmarks, ranging from 150 to 500 m in diameter (Fig. 1B), which agree well with densely developed NNE–SSW trending folds and faults on the spur (Okamura et al., 1994).

4. Sampling and analytical methods

In this study, close to 100 pore water samples were collected from 14 piston core sites throughout the research area. The piston cores ranged in length between 6 to 12 m and the cores were cut into 1 m-long whole round sections immediately after core recovery. These cores were subsectioned into 10 to 20 cm-long intervals, each of which was shaved to remove potential contamination. The subsections were squeezed to extract pore water at intervals of 25 cm in the upper 5 m and of 50 cm thereafter for UT04 cores and at intervals of 50 cm for all cores from KY05-08 using a shipboard Manheim hydraulic squeezer (Manheim et al., 1994) with a 0.45 μm disk filter. We selected 14 sites from the sample locations; PC09UT and 14UT during UT04 and PC02, 04, 05, 08, and 13 during KY05-08 from the Umitaka Spur, PC10, 11, and 12 (KY05-08) from the Joetsu Knoll, and PC06, 07, 14, and 15 (KY05-08) from the lower flank of the Umitaka Spur, summit of the eastern ridge, and the Joetsu Basin as references away from gas venting, near-surface gas hydrate, and BSRs (Fig. 1B). Individual pore water samples ranged between 5 and 10 ml of fluid and were sealed in plastic vials immediately after recovery for onshore geochemical analyses.

Dissolved Cl concentrations were measured with an ion chromatograph (IC), Dionex ICS-1000, and total Br and I concentrations were measured by inductively coupled plasma mass spectrometer (ICP-MS), Thermo Elemental X7 at the Cosmogenic Isotope Lab, University of Rochester. These values were determined against standard seawater from the International Association for the Physical Sciences of the Ocean (IAPSO) (Burton, 1996), with analytical precisions of better than 1% for the IC and 3% for the ICP-MS, respectively. While typically ~1 mg of I is sought for an AMS determination, Lu et al. (in press) reported that as low as 0.05 mg of I is sufficient for successful ^{129}I/I determinations with AMS, which allowed us to prepare targets from individual pore water samples. We selected a total of 20 samples from sites PC09UT and 14UT (UT04), PC05, 06, 07, 12, and 15 (KY05-08) for the measurements based on the iodine concentrations in the pore waters. Dissolved iodine was precipitated as AgI following the method outlined by Fehn et al. (1992). Iodate in the sample water was reduced to iodine by sodium bisulfite, and preconcentrated with anion resin. The purified iodine was extracted into chloroform, back extracted into sodium bisulfite, and then precipitated as AgI with silver nitrate. The ^{129}I/I ratios of these AgI targets were determined with the AMS system at the PRIME Lab, Purdue University (Sharma et al., 2000).

5. Results

Analytical results are listed in Table 1 and the depth profiles of pore water geochemistry are illustrated in Fig. 2. The downward patterns of Cl concentrations of sites with BSRs present vary between sites, while those at the reference sites remain almost constant at the IAPSO

Table 1
Analytical results of pore waters from the Umitaka Spur–Joetsu Knoll gas hydrate field near Sado Island in the eastern margin of the Japan Sea

Site (water depth)	Sample ID	Depth (mbsf)	Cl (mM)	Br (μM)	I (μM)	$^{129}I/I$ (10^{-15})
Seawater	IAPSO		546.0 [a]	837.6[a]	0.4[a]	1500±150 [b, c]
UT04						
PC09 (937 m)	S2-30	0.08	595.8	925.4	6.5	
	S2-60	0.38	603.6	940.0	13.6	
	S2-85	0.63	606.1	943.2	18.0	
	S3-0	0.78	612.2	945.8	19.8	
	S3-25	1.03	602.9	951.9	23.0	
	S3-50	1.28	605.5	950.0	25.3	1180±100
	S3-75	1.53	623.2	940.9	27.9	
	S4-0	1.78	614.8	963.2	29.5	
	S4-25	2.03	624.9	969.8	31.9	
	S4-50	2.28	634.8	984.4	33.9	
	S4-75	2.53	634.3	982.3	36.3	
	S5-0	2.78	635.5	991.2	38.5	
	S5-50	3.28	639.9	1001.4	43.1	690±100
	S6-0	3.78	638.4	1005.9	45.7	
	S6-50	4.28	644.9	1017.1	47.5	
PC14 (910 m)	S2-50	0.00	553.7	923.0	7.6	
	S2-75	0.25	562.4	945.7	18.3	
	S3-0	0.50	561.6	960.2	22.9	
	S3-25	0.75	566.1	969.5	32.1	
	S3-50	1.00	551.0	957.3	36.7	
	S3-75	1.25	555.7	968.8	41.4	960±140
	S4-0	1.50	545.9	982.3	49.4	
	S4-25	1.75	546.4	988.8	54.5	
	S4-50	2.00	541.2	972.8	57.9	
	S4-75	2.25	543.9	995.5	66.5	
	S5-0	2.50	542.3	996.2	71.8	
	S5-50	3.00	539.9	996.4	79.4	450±40
	S6-0	3.50	535.1	1003.6	86.1	
	S6-50	4.00	532.9	1007.7	92.3	
KY05-08						
PC02 (905 m)	F-btm (GH)	0.27	300.4	568.0	1.1	
	F-75	0.04	533.4	943.5	2.1	
	G-30	0.59	545.7	971.1	3.0	
	H-56	1.39	536.9	951.1	5.5	
	I	2.38	447.8	797.7	2.1	
	J-55	3.23	399.2	725.3	2.9	
PC04 (917 m)	F-30	0.02	534.7	931.0	3.7	
	G-50	1.22	550.9	967.1	21.3	
	H-50	2.20	574.2	1017.7	32.8	
	I-50	3.20	584.3	1110.2	44.0	
	J-50	4.19	591.2	1126.9	50.3	
	K-50	5.19	609.3	1174.0	55.1	
	L-50	6.19	625.8	1200.9	57.2	
PC05 (904 m)	D-24	0.00	536.9	1000.2	5.9	
	E-50	1.25	525.1	1030.7	38.3	800±400
	F-50	2.26	510.1	1064.1	65.0	
	G-50	3.29	497.3	1096.9	92.5	750±70
	H-50	4.29	485.7	1095.1	109.6	490±80
	I-50	5.29	467.8	1127.4	130.3	600±80
	J-50	6.29	447.6	1121.4	142.9	310±40
	K-50	7.29	441.5	1141.2	158.3	
	L-50	8.15	439.4	1167.8	170.6	400±30

Table 1 (*continued*)

Site (water depth)	Sample ID	Depth (mbsf)	Cl (mM)	Br (μM)	I (μM)	$^{129}I/I$ (10^{-15})
PC06 (1064 m)	C-40	0.04	542.9	1033.0	6.5	
	D-50	1.14	545.8	1058.3	33.4	1000±500
	E-50	2.14	540.1	1075.8	54.3	
	F-50	3.14	547.2	1121.4	77.2	650±70
	G-50	4.14	531.3	1122.2	95.9	
	H-50	5.14	540.8	1171.5	111.3	550±50
PC07 (1034 m)	C-52	0.00	553.3	1044.5	5.2	
	D-50	0.98	537.3	1064.3	27.0	
	E-50	1.99	547.2	1100.1	47.0	900±500
	F-50	2.99	539.2	1108.2	64.7	
	G-50	3.99	529.9	1116.9	83.3	
	H-50	4.99	521.8	1142.7	96.5	630±80
PC08 (888 m)	A-75	0.03	546.6	1011.7	2.2	
	B-20	0.37	547.4	1019.7	3.3	
	D-50	0.60	528.7	997.4	4.2	
	E-top (GH)	0.71	70.6	161.5	0.5	
PC10 (976 m)	B-85	0.07	547.9	1038.0	2.4	
	C-50	0.72	572.7	1080.8	2.8	
	D-50	1.72	632.2	1170.5	3.8	
	E-50	2.72	697.7	1290.6	4.9	
	F-50	3.42	797.8	1437.1	6.9	
PC11 (991 m)	F-top (GH)	1.19	47.6	113.0	0.4	
	F-btm (GH)	2.19	46.9	112.0	0.5	
PC12 (1111 m)	F-50	1.07	553.3	1105.4	48.3	
	G-50	2.08	523.4	1158.5	102.7	
	H-50	3.11	519.9	1240.4	158.9	500±100
	I-40	4.01	479.8	1167.5	150.3	430±70
PC13 (900 m)	E-70	0.57	558.7	1031.5	2.0	
	F-40	1.08	283.3	570.7	1.5	
	G-1	1.69	237.4	486.1	1.7	
	G-15 (GH)	1.83	81.5	183.5	0.8	
	G-50	2.18	346.1	676.0	2.4	
	G-70	2.28	296.3	588.8	3.4	
	H-30	2.98	354.9	691.5	2.7	
	H-35 (GH)	3.03	305.9	600.8	2.1	
	H-65	3.33	434.2	818.8	3.1	
PC14 (1021 m)	C-10	0.08	545.1	1014.2	5.0	
	C-50	0.48	547.3	1016.5	8.7	
	D-50	1.48	550.8	1025.2	16.6	
	E-50	2.48	549.7	1044.0	24.9	
PC15 (1027 m)	D-50	0.20	554.5	1023.7	6.6	
	E-50	1.30	549.3	1024.2	33.0	
	F-50	2.32	548.3	1040.0	51.0	680±170
	G-50	3.35	531.3	1068.1	65.3	
	H-50	4.36	530.5	1087.1	80.3	770±90
	I-50	5.36	525.4	1096.9	92.2	
	J-50	6.36	536.5	1105.1	99.8	580±160

mbsf = meters below sea-floor.
GH: massive gas hydrate sample.
[a] International Association for the Physical Sciences of the Ocean (IAPSO) standard seawater (Burton, 1996).
[b] Moran et al. (1998).
[c] Fehn et al. (in press).

standard seawater value, 546 mM (dashed line in Fig. 2). Several of the cores had sediments with visible gas hydrate occurrences and pore waters from those cores (PC02, 08, 11, and 13; solid symbols) are commonly diluted compared to the samples from cores without direct indication of gas hydrate presence. In contrast to the differences between the three sites observed in the behavior of Cl, Br and I patterns at all sites are very

similar; they increase rapidly downward to comparable concentrations, reaching 1000 to 1500 μM of Br and 150 to 200 μM of I at the bottom level of the cores, respectively. While both elements have concentrations considerably above that of standard seawater (Br=837.6 μM, I=0.4 μM; dashed lines in Fig. 2), as is typical for other gas hydrate fields, the enrichment of iodine is much more pronounced than that of bromine.

In subsets from seven cores, ^{129}I/I ratios were determined. All ratios are below the pre-anthropogenic value of $^{129}I/I = 1500 \times 10^{-15}$ (dashed line in Fig. 2; Moran et al., 1998; Fehn et al., in press), demonstrating the absence of anthropogenic ^{129}I in these fluids. The depth profiles of ^{129}I/I ratios are very similar at all sites; decreasing rapidly from $\sim 1200 \times 10^{-15}$ at <2 mbsf to between $\sim 400 \times 10^{-15}$ and $\sim 600 \times 10^{-15}$ at >4 mbsf.

6. Discussion

6.1. Geochemical characteristics of pore waters

6.1.1. Concentration profiles

The Cl concentrations in the pore waters collected from gas hydrate-bearing sediments can be strongly

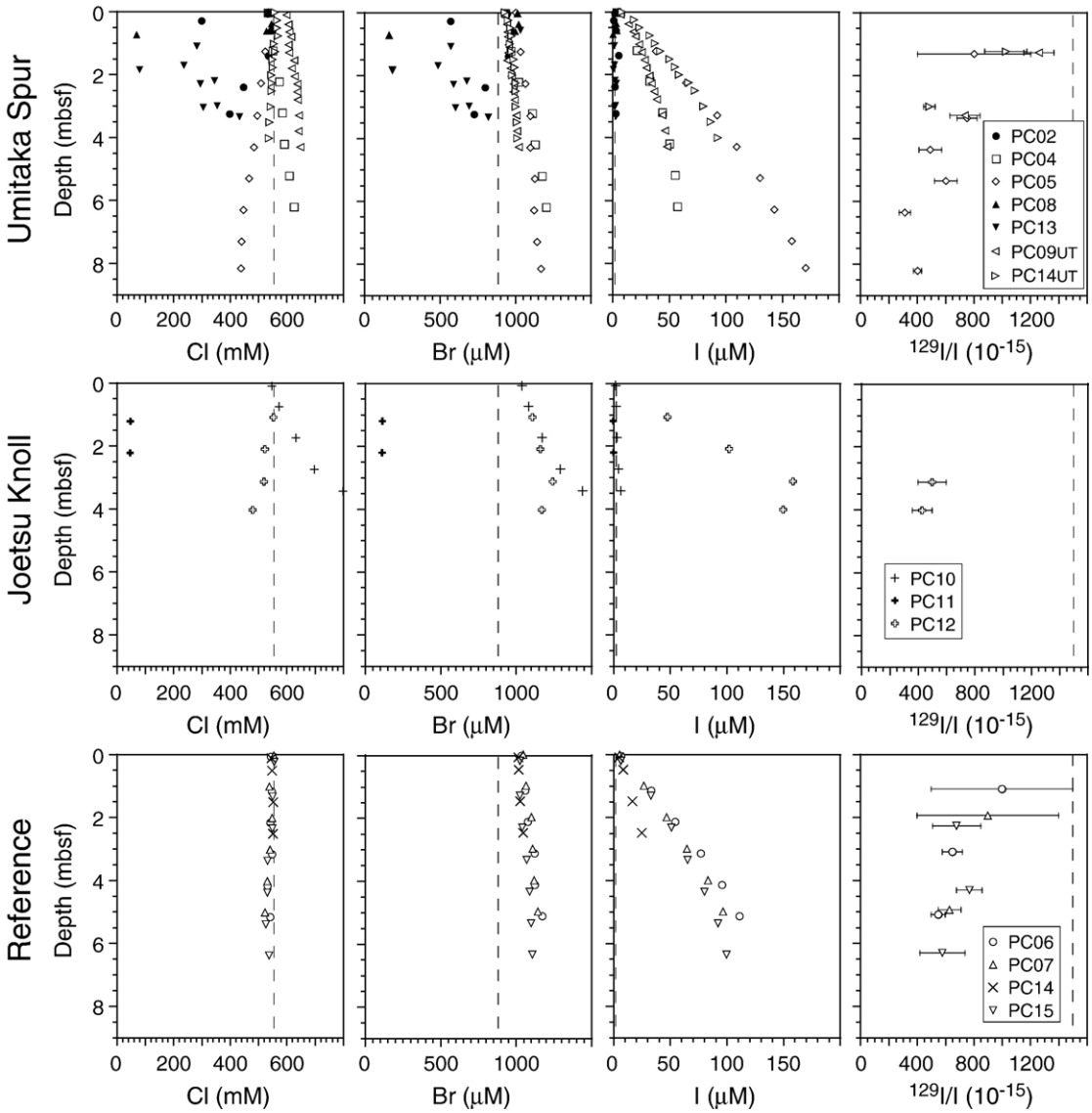

Fig. 2. Depth profiles of Cl, Br, and I concentrations and ^{129}I/I ratio at the Umitaka Spur, the Joetsu Knoll, and reference sites. Detailed sampling locations are shown in Fig. 1B. Gas hydrate-bearing cores are represented by solid symbols (sites PC02, PC08, PC11, and PC13). Dashed lines indicate seawater values for halogen concentrations (IAPSO) and ^{129}I/I (Moran et al., 1998; Fehn et al., in press).

modified by the input of the fresh water from dissociated gas hydrates during core recovery (e.g. Hesse, 2003; Tomaru et al., 2004), which results in discrete dilution of pore waters as observed at PC02, 08, 11, and 13. On the other hand, the Cl concentration of marine pore water can be gradually decreased by the input of diagenetic fresh water, derived from processes such as biogenic opal recrystallization, clay mineral dehydration, and clay membrane filtration (e.g. Kastner et al., 1991; Brown et al., 2001) or can be increased by the input of evaporated seawater or saline water from halite deposits (e.g. McCaffrey et al., 1987; Vengosh et al., 2000). In the gas hydrate field, however, the variation of Cl depth profiles can be modified by fluid input from the loci of gas hydrate deposits (Hiruta et al., 2005; Matsumoto et al., 2005). Both increase and decrease of Cl concentrations can be related to processes occurring during formation and dissociation of gas hydrates. Since fluids entering gas hydrate locations often have Cl concentrations below that of seawater (e.g. Egeberg and Dickens, 1999; Tomaru et al., 2006b), profiles often reflect the mixing of deep fluids with seawater near the seafloor. The observed gradual Cl decrease to ~440 mM can also be caused, however, by the dissociation of gas hydrate releasing fresh water at depths (e.g. Hesse, 2003), while the Cl increase to ~800 mM can be explained by the rapid formation of massive gas hydrate excluding saline residual water (Milkov et al., 2004; Torres et al., 2004). If that is the case, the steeper Cl gradient at PC10 at the Joetsu Knoll may reflect brine input from a large quantity of massive gas hydrate and/or the formation of gas hydrates just below the cored depth.

Although, similar to Cl concentrations, Br and I concentrations at PC02, 08, 11, and 13 are anomalously decreased by the dissociation of massive gas hydrate, they increase rapidly at the reference sites as well as at the other sites of the Umitaka Spur and the Joetsu Knoll. This increase probably indicates that rising deep fluids are potentially enriched in Br and I throughout the research area. The similarity observed for Br and I profiles between sites is in contrast to strong differences in methane fluxes estimated from sulfate–methane interfaces (SMIs), which are at ~3.5 mbsf at the reference sites and at 1.5 to 2.5 mbsf at the Umitaka Spur and the Joetsu Knoll (Hiruta et al., 2005). This observation probably reflects migration of free methane separate from the fluids in the shallow intervals at the geologically uplifted areas, leading to active methane venting on the spur and the knoll. The Br and I concentrations of near-surface samples are still as high as 900 to 1000 μM and 2 to 7 μM, respectively, which, in the case of I, is more than one order of magnitude higher than the standard seawater value (0.4 μM). An extremely high dissolved methane concentration in seawater over this area, up to 160 nmol/L (Ishida et al., 2005), implies an association of methane release with that of Br- and I-rich deep fluids into the water column, a phenomenon observed also in other areas such as the Black Sea (e.g. Aloisi et al., 2004).

The Cl–Br (Fig. 3) and Cl–I (Fig. 4) diagrams show strong similarities except for the scales for Br and I, suggesting a positive linear correlation between Br and I at each site. The Cl depletions of hydrate-bearing samples correspond well to those of Br and I, the fraction of gas hydrate derived water (Cl=0 mM) in sample water reaches ~91% at PC11 as indicated by the arrows representing halogen dilution due to gas hydrate dissociation (Figs. 3 and 4). Although Br and I enrichments generally are attributed to the advection of deep fluids which have experienced degradation processes of organic materials, those in Cl-rich samples might also reflect the input of brines which were excluded from gas hydrate structures (Milkov et al., 2004; Torres et al., 2004). The samples from the Joetsu Knoll, PC10, are relatively enriched in Cl and plot well along the arrows representing halogen enrichment due to residual brine input from gas hydrate. Therefore, gas hydrate may exist below the cored depth at PC10, and might have modified substantially the pore waters at this site.

6.1.2. Halogens in massive gas hydrate

The comparison between the different sets of cores indicates that the presence of massive gas hydrate in the sediments influences the concentrations of halogens in the pore waters. We collected a few pieces of massive gas hydrates from the Umitaka Spur (PC02, 08, 13) and the Joetsu Knoll (PC11) in order to determine the actual presence of halogens within gas hydrate solids (Fig. 5). The six pieces were stored immediately after retrieval and halogen concentration were measured in the liquid resulting from the melting of the solid phases. The results of these determinations are included in Table 1 and identified by the letters “GH”. Because no specific measures were undertaken to remove associated pore waters from the pieces, it is likely that halogens from pore waters were present. The measured concentrations of these samples therefore can be considered maximum values for the presence of halogens in massive gas hydrates.

Of the six samples, four show very low concentrations of halogens, while the other two (PC02 F-btm; PC13 H-35) have concentrations only slightly lower than those in the adjoining pore waters. The latter two probably are strongly influenced by the presence of

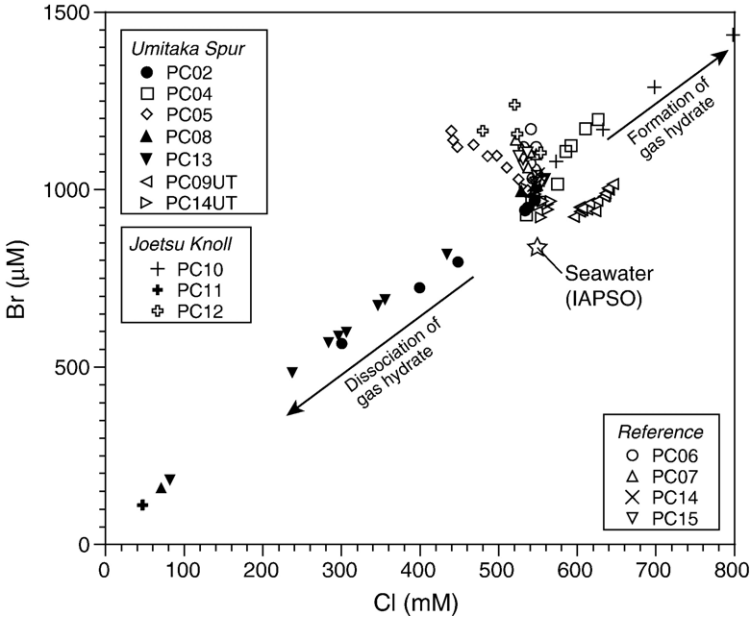

Fig. 3. Cl–Br diagram with arrows indicating Cl and Br enrichment and depletion due to gas hydrate formation and dissociation. Open star represents standard seawater (IAPSO) value.

pore waters and are not considered further for the discussion of halogens in solid gas hydrates. The concentrations in the remaining four samples are very similar with the following averages: Cl=61.6±17.2 mM; Br=142.5±35.8 μM, and I=0.55±0.17 μM. Compared to concentrations in pore waters at adjoining sites, massive gas hydrates contain still around 10% of Cl and Br, but less than 1% of I. At this point it is not clear whether halogens are incorporated into the crystal lattice or are found in fluid pockets trapped in the gas hydrates (e.g. Suess et al., 1999; Kuhs et al., 2004), but these data suggest that halogens are present at different

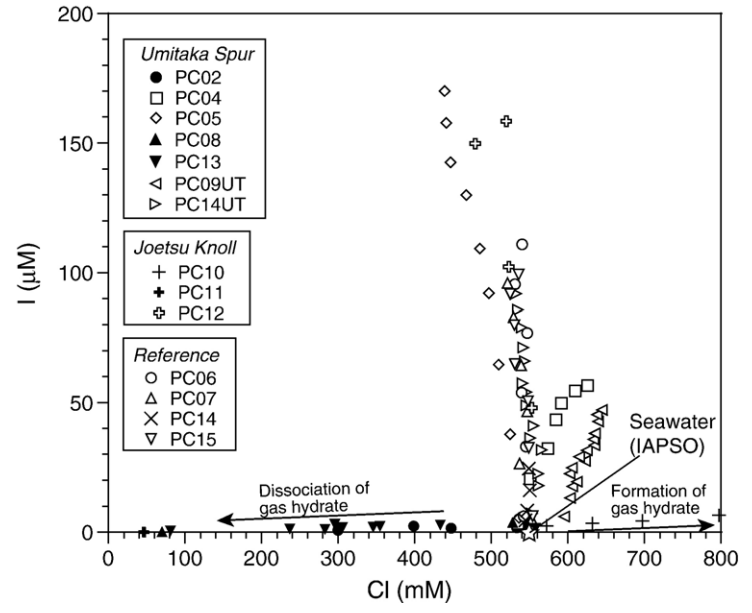

Fig. 4. Cl–I diagram with arrows indicating Cl and I enrichment and depletion due to gas hydrate formation and dissociation. Open star represents standard seawater (IAPSO) value.

concentrations in these solids. The release of fresh water from gas hydrates has thus a stronger effect on the concentration of I than on the concentrations of the other two halogens which leads to variations in element ratios in the pore fluids during the dissociation of gas hydrates. A detailed study of halogen concentrations in pore waters of the Nankai Trough gas hydrate fields shows this effect very convincingly (Muramatsu et al., 2006).

6.1.3. Halogen ratios in pore waters

The Cl-normalized Br and I values (Br/Cl and I/Cl molar ratios) demonstrate Br and I enrichment at all sites with respect to dilution or enrichment due to gas hydrate effects (Fig. 6). Compared to the ratios of standard seawater ($Br/Cl = 1.5 \times 10^{-3}$, $I/Cl = 7.3 \times 10^{-7}$; dashed lines in Fig. 6), deeper samples at all sites are enriched in Br and I by factors of > 2.3 and > 150, respectively, which reflect strong enrichment of these two biophilic halogens in rising deep fluids. Exceptions to this observation are the samples closely associated with gas hydrate-bearing layers which have considerably lower I/Cl and I/Br ratios than the other samples. Assuming that the juvenile water geochemistry at PC02 (gas hydrate-bearing sample) free from gas hydrate effects is close to that of adjoining PC04 (gas hydrate-free sample), Br and I at PC02 are depleted by ~12% and ~90%, respectively, compared to PC04. The similarity of these ratios in PC10 and those in sites with visible gas hydrate (PC02, 08, 13, and 11) suggests the presence of massive gas hydrate deposits near the cored intervals at PC10, although no direct gas hydrate proxies, as, for example, low temperature anomalies, degassing, or soupy texture, are observed in the recovered cores, which agree with the indication from Cl–Br (Fig. 3) and Cl–I (Fig. 4) diagrams.

Fig. 5. Photo of massive gas hydrate collected from PC11 at ~1.7 mbsf. Analytical results of melt waters from such gas hydrate samples are indicated as "GH" in Table 1.

In addition, the I/Cl and I/Br ratios of gas hydrate-bearing samples remain constant with depth. Pore waters within the massive gas hydrate interval are well mixed with seawater, resulting in low I/Cl and I/Br ratios, which may reflect a process by which massive gas hydrates prevent diffusion of deep fluids enriched in I and separate the water system above and below the gas hydrate layer. Shallow pore waters in the massive gas hydrate sites are dominated by seawater components.

6.1.4. Characterization of deep fluids

Several of the cores have Cl concentrations below that of seawater (Fig. 2). Two main explanations exist for the presence of Cl concentrations below seawater values; they can reflect either dilution with waters from the dissociation of gas hydrates or the presence of deep fluids which inherited their Cl depletion through other diagenetic processes. In the shallow intervals of PC02, 08, 11, and 13, dissociation of gas hydrates clearly is the cause for the low Cl concentrations. In these cores, the values show strong variations, concentrations of all three halogens are lowered, although at somewhat different rates, which leads to changes in element ratios between the halogens. This process has also been observed in deep cores from the Nankai Trough (Muramatsu et al., 2006).

In cores with a relatively smooth decrease in Cl concentrations, such as PC05, 12, or 14UT, the situation can reflect the input of deep fluids with low Cl concentrations, accompanied by elevated levels of Br and I. Such fluids have been observed in several other gas hydrate sites, such as Blake Ridge (Egeberg and Dickens, 1999) or Hydrate Ridge (Fehn et al., 2006) below the gas hydrate horizons. Because the profiles in our study area suggest further increases in Br and I (or decrease in Cl) concentrations with depth, the initial fluids probably have higher I and Br concentrations than observed here. Low Cl pore waters could, however, also be caused by the fresh water input from dissociated gas hydrates at depths (Hiruta et al., 2005; Matsumoto et al., 2005). If that is the case, the concentrations of all three halogens reflect values lower than the concentrations in the original fluids. Assuming that the original fluid in this case had Cl concentration similar to that of seawater, the initial values for the deepest section of PC05 would increase from 1200 to 1440 μM for Br and from 170 to 215 μM for I, for example. Because none of the cores comes close to reaching the lower limit of the gas hydrate zone, it is difficult to decide between these two explanations for decreases in Cl concentrations. In either case, however, the observed concentrations of Br and I constitute minimum values and the actual

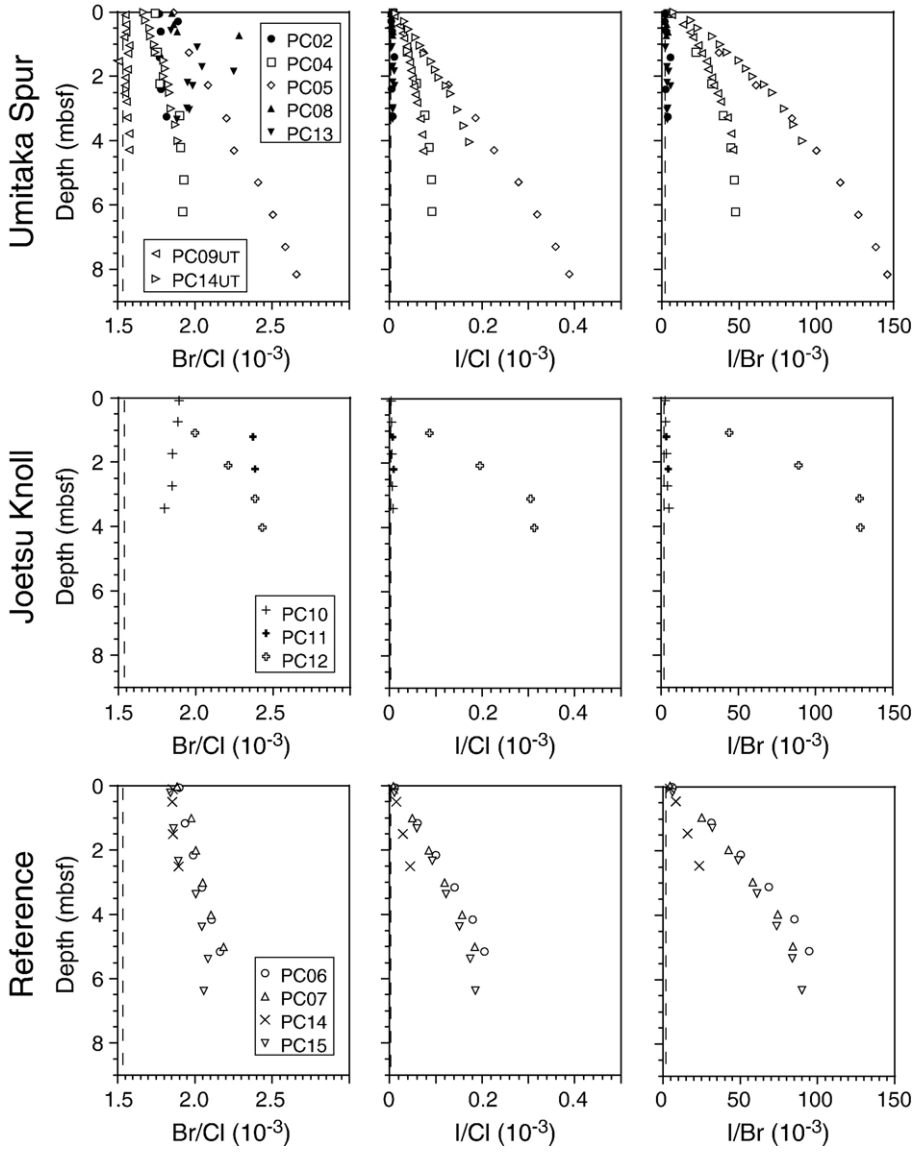

Fig. 6. Depth profiles of Br/Cl, I/Cl, and I/Br molar ratios. Dashed lines indicate the ratios of standard seawater (IAPSO), Br/Cl = 1.5×10^{-3}, I/Cl = 7.3×10^{-7}, and I/Br = 4.8×10^{-4}.

concentrations for these two halogens probably are higher than observed here.

Some indication on the influence of deep gas hydrates can be derived from the comparison of halogen ratios in the cores. PC05, PC12, and PC14UT are relatively enriched in I (high I/Cl and I/Br ratios) compared to those at high Cl sites, PC04, PC09UT, and PC10 and the reference sites (Fig. 6). If the iodine deviation is directly related to the occurrence of gas hydrates, iodine concentrations should be high in areas with gas hydrates present. Since the I/Cl and I/Br ratios at high Cl sites (e.g. PC04, PC09UT, and PC10) are relatively low, the concentrations probably reflect dilution of I-rich deep fluids with seawater, while low I/Cl and I/Br ratios at sites with low Cl concentrations (e.g. PC02, 08, 11, and 13) probably indicate the presence of massive gas hydrates below the cored intervals.

6.2. $^{129}I/I$ ratios in pore waters

6.2.1. $^{129}I/I$ profiles

Because of the low I concentrations in the shallow depths, these samples generally produce small AgI targets for AMS analyses, which result in relatively large error

margins (Fig. 2). Nevertheless, all observed ^{129}I/I ratios show rapid decreases in the shallow intervals, reflecting upward migration of deep fluids with high I concentrations and ^{129}I/I ratios lower than the observed values, and mixing between the deep fluids and shallow fluids with low I concentrations and high ^{129}I/I ratios either in the form of shallow pore waters or seawater. Almost constant ^{129}I/I ratios below ~4 mbsf at all sites indicate that the low ^{129}I/I fluid domination starts at these depths.

6.2.2. Estimation of ^{129}I/I ratio of deep fluids

The I concentrations, except for gas hydrate-bearing samples, increase logarithmically with depth, whereas Br concentration increase only linearly, which may reflect the release of reduced I^- in the shallow sediments (Fig. 2). Shallow pore waters probably receive young I from seawater and shallow sediments with ages <30 kyr, which has a ^{129}I/I ratio similar to that in seawater. Assuming that bottom seawater contains quantities of I from deep buried sediments, the ^{129}I/I ratio of seawater might be decreased from 1500×10^{-15} (Moran et al., 1998; Fehn et al., in press) to 1180×10^{-15} (observed maximum ratio; Table 1). The solid lines in Fig. 7 exhibit mixing trends between the sample with the lowest ^{129}I/I ratio (310×10^{-15}; PC05 J-50) and the standard seawater (I=0.4 μM) with ^{129}I/I ratios of 1500 and 1180×10^{-15}, respectively (shade in Fig. 7). All samples fall into a field above the mixing lines, indicating that young iodine release from sediments in the upper few meters contributes to the iodine in the pore waters. The maximum gradient for the highest I concentration sample at PC05 (dashed line in Fig. 7) suggests that the maximum I contribution from sediments ranges between 63.3 (^{129}I/I=1500×10^{-15}) and 77.5 μM (^{129}I/I=1180×10^{-15}). In addition, these extrapolations indicate that I concentrations and ^{129}I/I ratios of deep fluids rising into the cored depth interval are ~185 μM and 300×10^{-15}, respectively.

Because decomposition of organic materials at depths liberates I together with Br, the depth pattern of I is commonly similar to that of Br except for those at shallow depths, e.g. these concentrations rapidly increase with depth and reach maximum or constant values at the same depth (e.g. Egeberg and Dickens, 1999; Fehn et al., 2006; Muramatsu et al., 2006). Diagenetic release of Br occurs predominantly at depths and is negligible compared to the release of I in shallow sediments. Therefore, the effect of young I addition to the deep fluid on the ^{129}I/I depth profile can be estimated by subtracting the volume fraction of deep fluid calculated from Br concentrations at depths where stable concentrations have been reached. Assuming that the observed Br concentration (Br_{obs}) results only from mixing between Br in the deep fluid (Br_{df}) and in seawater (Br_{sw}), Br_{obs} can be described using the fraction of deep fluid (f) as:

$$Br_{obs} = f \cdot Br_{df} + (1-f) \cdot Br_{sw}. \quad (1)$$

Because the Br concentration increases linearly with depth (Fig. 2), f can be a function of depth. For I concentration (or the ^{129}I/I ratio) profile, therefore, f also represents the fraction of I (^{129}I) from deep fluids, while $(1-f)$ gives the fraction of "excess" I (^{129}I) from seawater and diagenesis of shallow sediments. The estimated ^{129}I/I ratio (R_{est}) including such I can then be expressed in the following equation:

$$R_{est} = \frac{f \cdot I_{df} \cdot R_{df} + (1-f) \cdot I_{sf} \cdot R_{sf}}{f \cdot I_{df} + (1-f) \cdot I_{sf}} \quad (2)$$

where I_{df} and R_{df} are I concentration and ^{129}I/I ratio of rising deep fluid into the cored interval and I_{sf} and R_{sf} are additions from seawater and sediments combined in the shallow interval (shallow fluid), respectively. Although the R_{sf} value can be constant in the sampled interval, 1500×10^{-15}, I_{sf} values probably vary with depth. However, the maximum effects of the shallow I can be calculated using Br_{df}=1500 μM, I_{sf}=63.3 μM, $R_{sf}=1500\times10^{-15}$ (or I_{sf}=77.5 μM, $R_{sf}=1180\times10^{-15}$), I_{df}=185 μM, and $R_{df}=300\times10^{-15}$ (estimated from Fig. 7). Fig. 8 shows the results of estimated R_{est} profiles on the observed ^{129}I/I ratios at sites PC05 and PC15 (shade bounded by solid lines). In the very shallow intervals where observed I concentrations are below I_{sf}, mixing with seawater (I=0.4 μM) is applied (shade bounded by dashed lines). Although the observed ^{129}I/I ratios at PC15 agree well with the estimated pattern, those at PC05 are still smaller, which reflects smaller effects of shallow I at PC05 (Umitaka Spur) than at PC15 (reference), i.e. deep fluid flux is greater at the spur than at the reference site. Rapid ^{129}I/I changes due to I derived from young sediments and seawater occur only in the very shallow intervals, and the ^{129}I/I ratios of samples below 5 to 6 mbsf represent well the ratio in the rising deep fluid, because I concentrations of deep fluids are much greater than that in the shallow fluids. The ^{129}I/I ratios in this area thus fall into the observed range between $\sim400\times10^{-15}$ at the Umitaka Spur and the Joetsu Knoll and $\sim600\times10^{-15}$ at the reference sites (Fig. 2).

6.3. Potential iodine age signal

The elapsed time (t) since the ^{129}I was isolated from the equilibrated iodine budget, i.e. seawater, can be

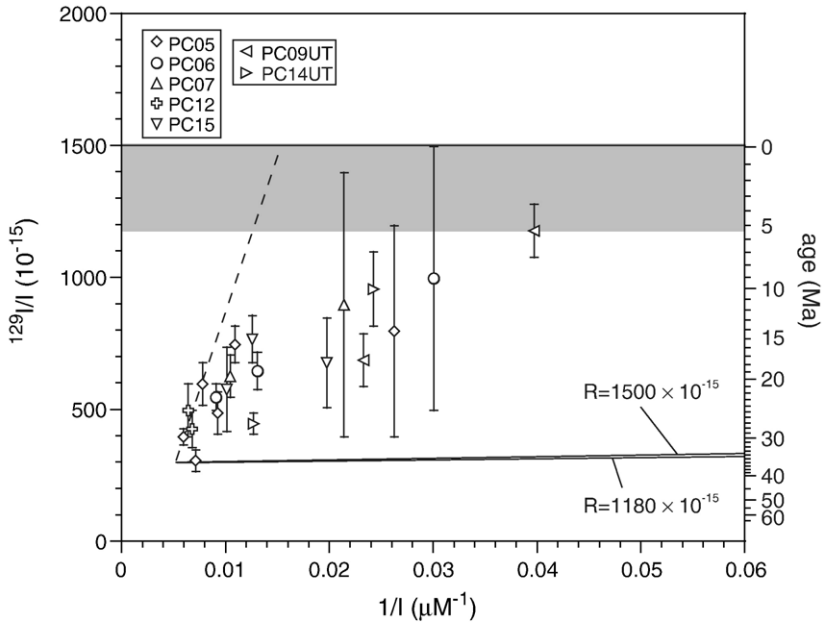

Fig. 7. Mixing diagram for ^{129}I/I with shade indicating probable ^{129}I/I range of seawater (1500×10^{-15}; Moran et al., 1998; Fehn et al., in press) and fluid from shallow sediments (1180×10^{-15}; PC09UT S3-50). Solid lines represent mixing between the lowest ^{129}I/I sample (PC05 J-50) and standard seawater (I=0.4 μM) with ^{129}I/I of 1500×10^{-15} or 1180×10^{-15}. Dashed line shows input of possible highest I fluid from sediments, the estimated I concentration is 63.3 μM at ^{129}I/I=1500×10^{-15} and 77.5 μM at ^{129}I/I=1180×10^{-15}. The intersection point at I concentration of 185 μM and ^{129}I/I ratio of 300×10^{-15} indicates I composition of initial deep fluid.

calculated by the observed radio/stable isotopic ratio (^{129}I/I) of iodine (R_{obs}) and the standard decay equation:

$$R_{obs} = R_0 e^{-\lambda_{129} t} \quad (3)$$

where R_0 is the initial seawater ^{129}I/I ratio of 1500×10^{-15} (Moran et al., 1998; Fehn et al., in press), and λ_{129} is the decay constant of ^{129}I (4.41×10^{-8} yr^{-1}). Therefore, the elapsed time, t, suggests an iodine age of ~30 Ma at the Umitaka Spur and the Joetsu Knoll (^{129}I/I=400×10^{-15}), and ~20 Ma at the reference sites (^{129}I/I=600×10^{-15}), suggesting that the source formations for the iodine are of Late Oligocene to Early Miocene age. The oldest ages within that range are found at the active methane venting areas.

Because spontaneous fission of ^{238}U in the entire sediment column produces ^{129}I during fluid migration particularly in the porous sediments, the observed ^{129}I/I ratio has been possibly increased and the iodine age can be underestimated. The total fissiogenic ^{129}I production is calculated as (Snyder and Fabryka-Martin, 2006):

$$N_{129} = N_{238}\lambda_{238}Y_{129}\varepsilon\rho\{(1-\varphi)/\varphi\}(1-e^{-\lambda_{129}t})/\lambda_{129} \quad (4)$$

where N_{129} and N_{238} are the number of ^{129}I and ^{238}U atoms, λ_{238} and λ_{129} are the decay constants for spontaneous fission of ^{238}U (8.5×10^{-17} yr^{-1}) and ^{129}I (4.4×10^{-8} yr^{-1}), Y_{129} is production yield for mass 129 (3.0×10^{-4}; Hebeda et al., 1987), ε is the escape efficiency of ^{129}I from the mineral lattice into the fluid, ρ is the rock density, φ is the effective porosity. The potential input of fissiogenic ^{129}I can be calculated assuming the following values for these parameters; N_{238}=6 ppm (Klinkhammer and Palmer, 1991; Gariepy et al., 1993) and ε=1 (Fabryka-Martin et al., 1989; Fehn et al., 1992, 2000; Moran et al., 1995), typical for deep sediments; ρ=2.7 g/cm^3, and φ=0.4. Based on these values, the observed ^{129}I/I ratios can be increased by 70×10^{-15} due to the fissiogenic input, which is well within the error margin of the results.

The obtained iodine ages correspond well with the age range of rapid deposition caused by the rifting along the margins due to oblique plate motions at <~28 Ma (Yamaji, 1990; Tamaki et al., 1992; Taira, 2001) and the rotation of NE and SW geological parts of Japan initiated at ~18 Ma, followed by seawater invasion from Pacific Ocean through the Fossa Magna (Kato, 1992; Jolivet et al., 1994). The Early Miocene formations in this area, e.g. Moriya, Uchiyama, Kanose, Tsugawa, and Nanatani Formations (Tanaka et al., 1962; Yamagishi, 1964; Yoshimura and Ishibashi, 1979; Kato, 1992), consist mostly of shallow marine sediments with

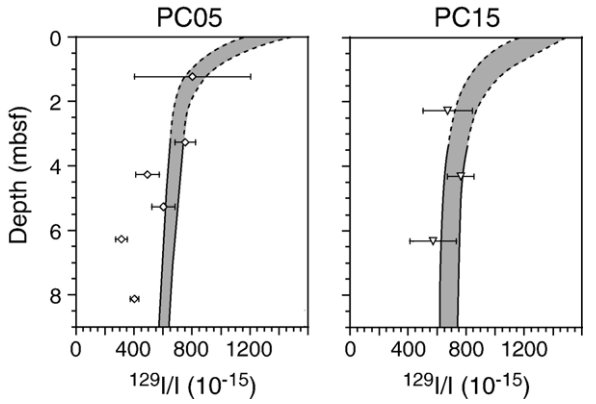

Fig. 8. Expected ^{129}I/I depth profiles showing mixing between deep fluid and young I released from local sediments. To provide maximum effects of young I, mixing between deep fluid (I_{df}=185 M, $R_{df}=300\times10^{-15}$) and shallow fluid (I_{sf}=63.3 μM, $R_{sf}=1500\times10^{-15}$ or I_{sf}=77.5 μM, $R_{sf}=1180\times10^{-15}$) is assumed for the samples with I concentration of >77.5 μM (depth intervals indicated by solid lines). For samples with I concentration of <77.5 μM, mixing between deep fluid and standard seawater (I=0.4 μM) is assumed (indicated by dashed lines). Depth profile of deep fluid fraction is calculated from deviation of Br concentration from the standard seawater value, increasing with depth.

altered pyroclastic rocks called Green Tuff which formed by the intensive eruptions of submarine volcanoes associated with the spreading of the Japan Sea. The source formations responsible for iodine and methane generations are probably local, underlying this area. The observation that iodine ages at the active methane venting sites are ~10 Myr older than those at the reference sites suggests that fluid regimes in this area are largely independent and derive methane from different source formations.

The source formation of iodine associated with active methane venting in the Umitaka Spur–Joetsu Knoll gas hydrate field is correlated well with the depositional system led by the early geological movements forming the Japanese Island Arc. In contrast, the iodine ages of pore waters in the Nankai Trough gas hydrate field in the fore arc setting of the Japanese Island Arc, where gas hydrates accumulate preferentially in sandy formations with saturations >80% of pores (Matsumoto et al., 2004; Tsuji et al., 2004), are predominantly >30 Ma at 26 to 223 mbsf, representing iodine migration from older formations in the continental side (Fehn et al., 2003). The contrast of source formations of iodine between gas hydrate fields in the Japan Sea and the Nankai Trough exhibits well the difference of methane accumulation models: methane derived over short distances from a rapidly deposited system associated with the expansion of a back arc basin, versus long distance migration of methane through the accretion-related deformed system in the fore arc setting along the Japanese Island Arc.

7. Conclusion

Pore waters were collected from an actively venting gas hydrate field near Sado Island, specifically from the Umitaka Spur–Joetsu Knoll area of this field, located at the eastern margin of the Japan Sea. Downward profiles of Cl suggest the input of residual brine from the formation of near-surface massive gas hydrate and possibly of fresh water from the dissociation of deep-seated disseminated gas hydrate. In contrast to the Cl profiles, at all sites Br and I concentrations are higher than that of seawater and increase with depth. This increase indicates the upward migration of deep fluids enriched in I and Br as well as methane in this area. Exceptions to these observations are sites where massive gas hydrates are present near the surface. In these sites, Br and I variations are considerably reduced, indicating low water permeability led by the formation of dense massive gas hydrate.

The ^{129}I/I ratios in all samples are below the pre-anthropogenic marine ratio of $R_0=1500\times10^{-15}$. The profiles show a decrease in ratio from samples close to the sediment–seawater interface with depth, indicating mixing of deep fluids with near-surface pore waters. The initial ^{129}I/I ratio of deep pore fluid is estimated to be $\sim400\times10^{-15}$ at the active venting sites and $\sim600\times10^{-15}$ at the reference sites. These ratios correspond to ages of 30 Ma and 20 Ma for the potential I source formations, respectively, suggesting that the I associated with active venting is essentially older than that at the area lacking venting and/or gas hydrate. Overall, the obtained age range corresponds well with the age when the opening of the Japan Sea was initiated at <28 Ma, followed by the rotation of NE and SW geological parts of Japan forming the Fossa Magna sedimentary basin at ~18 Ma. The close association between iodine and methane in aqueous solution makes it likely that the organic-rich source formations for iodine also provide the majority of methane in this area. Our results indicate that methane in the Umitaka Spur and Joetsu Knoll gas hydrate field is principally associated with the tectonic processes forming the Japan Sea called Green Tuff movement and that the gas hydrate fields near Sado Island derive most of their methane from deep sources formed during the opening of the Japan Sea.

Acknowledgements

We thank the crew of research vessels, Umitaka-maru of the Tokyo University of Marine Science and

Technology and Kaiyo of JAMSTEC. We also appreciate the collaboration with Y. Okuda and M. Satoh, National Institute of Advanced Industrial Science and Technology, T. Goto and H. Machiyama, JAMSTEC, and our colleagues during the cruises. We are grateful for iodine isotope determination carried out at the PRIME Lab, Purdue University, by D. Elmore, M. Caffee and their group. The authors are also grateful for helpful comments and insights provided by two anonymous reviewers. This study was supported by Grant-in-Aid from the Ministry of Education, Culture, Sports, Science and Technology (MEXT) to R. Matsumoto (No. 1620-1002), NSF Grant OCE-0550122 to U. Fehn, and the Postdoctoral Fellowship for Research Abroad from the Japan Society for the Promotion of Science (JSPS) to H. Tomaru.

References

Aloisi, G., Drews, M., Wallmann, K., Bohrmann, G., 2004. Fluid expulsion from the requirements mud volcano (Black Sea) Part I. Fluid sources and relevance to Li, B, Sr, I and dissolved inorganic nitrogen cycles. Earth and Planetary Science Letters 225, 347–363.

Aoyama, C., Matsumoto, R., Okuda, Y., Ishida, Y., Hiruta, A., Sunamura, M., Numanami, H., Tomaru, H., Snyder, G.T., Komatsubara, J., Takeuchi, R., Hiromatsu, M., Aoyama, D., Koike, Y., Takeda, S., Hayashi, T., Hamada, H., Kawada, Y., 2005. Acoustical survey of methane plumes using the quantitative echo sounder in the eastern margin of the Sea of Japan. Proceedings of the Fifth International Conference on Gas Hydrate. Trondheim, Norway, pp. 790–795.

Broecker, W.S., Peng, T.H., 1982. Tracers in the Sea. Eldigio Press, Palisades, NY. 690 pp.

Brown, K.M., Saffer, D.M., Bekins, B.A., 2001. Smectite diagenesis, pore-water freshening, and fluid flow at the toe of the Nankai wedge. Earth and Planetary Science Letters 194, 97–109.

Burton, J.D., 1996. The ocean: a global geochemical system. In: Summerhayes, C.P., Thorpe, S.A. (Eds.), Oceanography: an Illustrated Guide. Manson, London, pp. 165–181.

Egeberg, P.K., Dickens, G.R., 1999. Thermodynamic and pore water halogen constraints on gas hydrate distribution at ODP Site 997 (Blake Ridge). Chemical Geology 153, 53–79.

Elderfield, H., Truesdale, V.W., 1980. On the biophilic nature of iodine in seawater. Earth and Planetary Science Letters 50, 105–114.

Elmore, D., Gove, H.E., Ferraro, R., Kilius, L.R., Lee, H.W., Chang, K.H., Beukens, R., Litherland, A.E., Russo, C.J., Purser, K.H., Murrell, M.T., Finkel, R.C., 1980. Determination of ^{129}I using tandem accelerator mass spectrometry. Nature 286, 138–140.

Fabryka-Martin, J.T., Bentley, H.W., Elmore, D., Airey, P.L., 1985. Natural iodine-129 as an environmental tracer. Geochimica et Cosmochimica Acta 49, 337–347.

Fabryka-Martin, J.T., Davis, S.N., Elmore, D., Kubik, P.W., 1989. In situ production and migration of ^{129}I in the Stripa granite: Sweden. Geochimica et Cosmochimica Acta 53, 1817–1823.

Fehn, U., Peters, E.K., Tullai-Fitzpatrick, S., Kubik, P.W., Sharma, P., Teng, R.T.D., Gove, H.E., Elmore, D., 1992. ^{129}I and ^{36}Cl concentrations in waters of the eastern Clear Lake Area, California: residence times and source ages of hydrothermal fluids. Geochimica et Cosmochimica Acta 56, 2069–2079.

Fehn, U., Snyder, G.T., Egeberg, P.K., 2000. Dating of pore waters with ^{129}I: relevance for the origin of marine gas hydrates. Science 289, 2332–2335.

Fehn, U., Snyder, G.T., Matsumoto, R., Muramatsu, Y., Tomaru, H., 2003. Iodine dating of pore waters associated with gas hydrates in the Nankai area, Japan. Geology 31, 521–524.

Fehn, U., Lu, Z., Tomaru, H., 2006. Data report: ^{129}I/I ratios and halogen concentrations in pore water of Hydrate Ridge and their relevance for the origin of gas hydrates: a progress report. In: Trehu, A.M., Bohrmann, G., Torres, M.E., Colwell, F.S. (Eds.), Proceedings of the Ocean Drilling Program, Scientific Results 204. Ocean Drilling Program, College Station, Texas, pp. 1–25.

Fehn, U., Moran, J.E., Snyder, G.T., Muramatsu, Y., in press. The initial ^{129}I/I ratio and the presence of 'old' iodine in continental margins. Nuclear Instruments and Methods in Physics Research B.

Gariepy, C., Ghaleb, B., Hillaire-Marcel, C., Mucci, A., Vallieres, S., 1993. Early diagenetic processes in Labrador Sea sediments: uranium-isotope geochemistry. Canadian Journal of Earth Sciences 31, 29–37.

Ginsburg, G.D., Milkov, A.V., Soloviev, V.A., Egorov, A.V., Cherkashev, G.A., Vogt, P.R., Crane, K., Lorenson, T.D., Khutorskoy, M.D., 1999. Gas hydrate accumulation at the Hakon Mosby Mud Volcano. Geo-Marine Letters 19, 57–67.

Haeckel, M., Suess, E., Wallmann, K., Rickert, D., 2004. Rising methane gas bubbles from massive hydrate layers at the seafloor. Geochimica et Cosmochimica Acta 68, 4335–4345.

Harvey, G.R., 1980. A study of the chemistry of iodine and bromine in marine sediments. Marine Chemistry 8, 327–332.

Hebeda, E.H., Schultz, L., Freundel, M., 1987. Radiogenic, fissiogenic, and nucleogenic noble-gases in zircons. Earth and Planetary Science Letters 85, 79–90.

Hensen, C., Wallmann, K., Schmidt, M., Ranero, C.R., Suess, E., 2004. Fluid expulsion related to mud extrusion off Costa Rica-A window to the subduction slab. Geology 32, 201–204.

Hesse, R., 2003. Pore water anomalies of submarine gas-hydrate zones as tool to assess hydrate abundance and distribution in the subsurface. What have we learned in the past decade? Earth-Science Reviews 61, 149–179.

Hiruta, A., Matsumoto, R., Ishida, Y., Tomaru, H., Snyder, G.T., Aoyama, C., Hiromatsu, M., 2005. Formation of gas hydrate and carbonate nodules around active seeps of thermogenic methane at eastern margin of Japan Sea. Eos, Transactions AGU 86 (Fall Meeting Supplement, Abstract OS43A-0613).

Ishida, Y., Matsumoto, R., Hiruta, A., Aoyama, C., Tomaru, H., Hiromatsu, M., 2005. High concentration of methane and magnificent gas plumes over gas hydrate field in the eastern margin of Japan Sea. Eos, Transactions AGU 86 (Fall Meeting Supplement, Abstract OS43A-0614).

Jolivet, L., Tamaki, K., 1992. Neogene kinematics in the Japan Sea region and volcanic activity of the northeast Japan arc. In: Tamaki, K., Suyehiro, K., Allan, J., McWilliams, M., et al. (Eds.), Proceedings of the Ocean Drilling Program. Scientific Results, vol. 127/128. Ocean Drilling Program, College Station, Texas, pp. 1311–1331.

Jolivet, L., Tamaki, K., Fournier, M., 1994. Japan Sea, opening history and mechanism: a synthesis. Journal of Geophysical Research 99, 22237–22259.

Kastner, M., Elderfield, H., Martin, J.B., 1991. Fluids in convergent margins: what do we know about their composition, origin, role in diagenesis and importance for oceanic chemical fluxes. Philosophical Transactions of the Royal Society. A 335, 243–259.

Kato, H., 1992. Fossa Magna-A masked border region separation southwest and north west Japan. Bulletin of the Geological Survey of Japan 43, 1–30.

Kennedy, H.A., Elderfield, H., 1987a. Iodine diagenesis in pelagic deep-sea sediments. Geochimica et Cosmochimica Acta 51, 2489–2504.

Kennedy, H.A., Elderfield, H., 1987b. Iodine diagenesis in non-pelagic deep-sea sediments. Geochimica et Cosmochimica Acta 51, 2505–2514.

Klinkhammer, G.P., Palmer, M.R., 1991. Uranium in the oceans: where it goes and why. Geochimica et Cosmochimica Acta 55, 1799–1806.

Kuhs, W.S., Genov, G., Goreshnik, E., Zeller, E., Techmer, K.S., Bohrmann, G., 2004. The impact of porous microstructures of gas hydrates on their macroscopic properties. In: Chung, J.S., Izumiyama, K., Sayed, M., Hong, S.W. (Eds.), The Fourteenth (2004) International Offshore and Polar Engineering Conference. Toulon, France, pp. 31–35.

Lu, Z., Fehn, U., Tomaru, H., Elmore, D., Ma, X., in press. Reliability of ^{129}I/I ratios produced from small sample masses. Nuclear Instruments and Methods in Physics Research B.

Manheim, F.T., Brooks, E.G., Winters, W.J., 1994. Description of a hydraulic sediment squeezer. U. S. Geological Survey Open-File Report, vol. 94-0584.

Matsubara, Y., Seno, T., 1980. Paleogeographic reconstruction of the Philippine Sea at 5 m.y. B.P. Earth and Planetary Science Letters 51, 406–414.

Matsumoto, R., Tomaru, H., Lu, H., 2004. Detection and evaluation of gas hydrates in the eastern Nankai Trough by geochemical and geophysical methods. Resource Geology 54, 53–67.

Matsumoto, R., Okuda, Y., Aoyama, C., Hiruta, A., Ishida, Y., Sunamura, M., Numanami, H., Tomaru, H., Snyder, G.T., Komatsubara, J., Takeuchi, R., Hiromatsu, M., 2005. Methane plumes over a marine gas hydrate system in the eastern margin of Japan Sea: a possible mechanism for the transportation of subsurface methane to shallow waters. Proceedings of the Fifth International Conference on Gas Hydrate. Trondheim, Norway, pp. 749–754.

Mazurenko, L.L., Soloviev, V.A., Gardner, J.M., Ivanov, M.K., 2003. Gas hydrates in the Ginsburg and Yuma mud volcano sediments (Moroccan Margin): results of chemical and isotopic studies of pore water. Marine Geology 195, 201–210.

McCaffrey, M.A., Lazar, B., Holland, H.D., 1987. The evaporation path of seawater and the coprecipitation of Br^- and K^+ with halite. Journal of Sedimentary Petrology 5, 928–937.

Milkov, A.V., Dickens, G.R., Claypool, G.E., Lee, Y.-J., Borowski, W.S., Torres, M.E., Xu, W., Tomaru, H., Trehu, A.M., Schultheiss, P., 2004. Co-existence of gas hydrate, free gas, and brine within the regional gas hydrate stability zone at Hydrate Ridge (Oregon margin): evidence from prolonged degassing of a pressurized core. Earth and Planetary Science Letters 222, 829–843.

Moran, J.E., Fehn, U., Hanor, J.S., 1995. Determination of source ages and migration patterns of brines from the U.S. Gulf Coast Basin using ^{129}I. Geochimica et Cosmochimica Acta 59, 5055–5069.

Moran, J.E., Fehn, U., Teng, R.T.D., 1998. Variations in ^{129}I/^{127}I ratios in recent marine sediments: evidence for a fossil organic component. Chemical Geology 152, 193–203.

Muramatsu, Y., Doi, T., Tomaru, H., Fehn, U., Takeuchi, R., Matsumoto, R., 2006. Halogen concentrations in pore waters and sediments of the Nankai Trough, Japan: Implications for the origin of gas hydrates. Applied Geochemistry (revised).

Muramatsu, Y., Wedepohl, K.H., 1998. The distribution of iodine in the earth's crust. Chemical Geology 147, 201–216.

Nakamura, K., 1983. Possible nascent trench along the eastern Japan Sea as the convergent boundary between Eurasian and North American plates. Bulletin of the Earthquake Research Institute, University of Tokyo 58, 711–722.

Okamura, Y., Takeuchi, K., Joshima, M., Satoh, M., 1994. Geological map of South of Sado Island (1:200,000). Marine Geology Map Series, 43. Geological Survey of Japan.

Okamura, Y., Watanabe, M., Morijiri, R., Satoh, M., 1995. Rifting and basin inversion in the eastern margin of the Japan Sea. Island Arc 4, 166–181.

Price, N.B., Calvert, S.E., 1977. The contrasting geochemical behaviors of iodine and bromine in recent sediments from the Namibian shelf. Geochimica et Cosmochimica Acta 41, 1769–1775.

Price, N.B., Calvert, S.E., Jones, P.G.W., 1970. The distribution of iodine and bromine in the sediments of the South Western Barents Sea. Journal of Marine Research 28, 22–34.

Sharma, P., Bourgeois, M., Elmore, D., Granger, D., Lipschutz, M.E., Ma, X., Miller, T., Mueller, K., Rickey, F., Simms, P., Vogt, S., 2000. PRIME lab AMS performance, upgrades and research applications. Nuclear Instruments & Methods in Physics Research. Section B, Beam Interactions With Materials and Atoms 172, 112–123.

Shoji, H., Soloviev, V., Matveeva, T., Mazurenko, L., Minami, H., Hachikubo, A., Sakagami, H., Hyakutake, K., Kaulio, V., Gladysch, V., Logvina, E., Obzhirov, A., Baranov, B., Khlystov, O., Biebow, N., Poort, J., Jin, Y.K., Kim, Y., 2005. Hydrate-bearing structures in the Sea of Okhotsk. Eos, Transactions, AGU 86, 13–24.

Snyder, G.T., Fabryka-Martin, J.T., 2006. ^{129}I and ^{36}Cl in dilute hydrocarbon waters: Marine cosmogenic, in situ, and anthropogenic sources. Applied Geochemistry (revised).

Suess, E., Torres, M.E., Bohrmann, G., Collier, R.W., Greinert, J., Linke, P., Rehder, G., Tréhu, A.M., Wallmann, K., Winckler, G., Zuleger, E., 1999. Gas hydrate destabilization: enhanced dewatering, benthic material turnover and large methane plumes at the Cascadia convergent margin. Earth and Planetary Science Letters 170, 1–15.

Taira, A., 2001. Tectonic evolution of the Japanese Island Arc system. Annual Review of Earth and Planetary Science 29, 109–134.

Tamaki, K., Honza, E., 1985. Incipient subduction and obduction along the eastern margin of Japan Sea. Tectonophysics 119, 381–406.

Tamaki, K., Suyehiro, K., Allan, J., Ingle, J.C., Pisciotto, K.A., 1992. Tectonic synthesis and implications of Japan Sea ODP Drilling. In: Tamaki, K., Suyehiro, K., Allan, J., McWilliams, M., et al. (Eds.), Proceedings of the Ocean Drilling Program. Scientific Results, vol. 127/128. Ocean Drilling Program, College Station, Texas, pp. 1333–1348.

Tanaka, K., Morozumi, S., Koike, H., Hatakoshi, T., 1962. On the Tertiary system around Mt. Moriya, Nagano Prefecture. Journal of Geological Society of Japan 68, 618–628.

Tomaru, H., Matsumoto, R., Lu, H., Uchida, T., 2004. Geochemical process of gas hydrate formation in the Nankai Trough based on chloride and isotopic anomalies in interstitial water. Resource Geology 54, 45–51.

Tomaru, H., Fehn, U., Lu, Z., Matsumoto, R., 2006a. Halogen systematics in the Mallik Gas Hydrate Well, Northwest Territories, Canada: Implications for the origin of gas hydrates under terrestrial permafrost conditions. Applied Geochemistry (revised).

Tomaru, H., Matsumoto, R., Torres, M.E., Borowski, W.S., 2006b. Geological and geochemical constraints on the isotopic

composition of interstitial waters from the Hydrate Ridge region, Cascadia continental margin. In: Trehu, A.M., Bohrmann, G., Torres, M.E., Colwell, F.S. (Eds.), Proceedings of the Ocean Drilling Program. Scientific Results, vol. 204. Ocean Drilling Program, College Station, Texas, pp. 1–20.

Torres, M.E., Wallmann, K., Tréhu, A.M., Bohrmann, G., Borowski, W.S., Tomaru, H., 2004. Gas hydrate growth, methane transport, and chloride enrichment at the southern summit of Hydrate Ridge, Cascadia margin off Oregon. Earth and Planetary Science Letters 226, 225–241.

Tréhu, A.M., Bohrmann, G., Rack, F.R., Collett, T.S., Goldberg, D.S., Long, P.E., Milkov, A.V., Riedel, M., Schultheiss, P., Torres, M.E., Bang, N.L., Barr, S.R., Borowski, W.S., Claypool, G.E., Delwiche, M.E., Dickens, G.R., Gracia, E., Guerin, G., Holland, M., Johnson, J.E., Lee, Y.-J., Liu, C.-S., Su, X., Teichert, B., Tomaru, H., Vanneste, M., Watanabe, M., Weinberger, J.L., 2004. Three-dimensional distribution of gas hydrate beneath southern Hydrate Ridge: constraints from ODP Leg 204. Earth and Planetary Science Letters 222, 845–862.

Tsuji, Y., Ishida, H., Nakamizu, M., Matsumoto, R., Shimizu, S., 2004. Overview of the MITI Nankai Trough wells: a milestone in the evaluation of methane hydrate resources. Resource Geology 54, 3–10.

Tsunogai, S., 1971. Iodine in the deep water of the ocean. Deep-Sea Research and Oceanographic Abstracts 18, 913–919.

Uchida, T., Lu, H., Tomaru, H., 2004. Subsurface occurrence of natural gas hydrate in the Nankai Trough area: implication for gas hydrate concentration. Resource Geology 54, 35–44.

Vengosh, A., Gieskes, J., Mahn, C., 2000. New evidence for the origin of hypersaline pore fluids in the Mediterranean basin. Chemical Geology 163, 287–298.

Yamagishi, I., 1964. Geology in the northern district of Ueda City, Nagano Prefecture, with special reference to Green Tuffs. Journal of Geological Society of Japan 70, 315–338.

Yamaji, A., 1990. Rapid intra-arc rifting in Miocene northeast Japan. Tectonics 9, 365–378.

Yoshimura, T., Ishibashi, E., 1979. Geology of the mouth area of the Hime River and the Itoigawa–Shizuoka Tectonic Line. Island Arc 111, 1–30 (disturbance report).